Experimental Laboratory Research

Ligand-Based Molecular MRI: O-17 JJVCPE Amyloid Imaging in Transgenic Mice

Kiyotaka Suzuki, PhD, Hironaka Igarashi, MD, PhD, Vincent J. Huber, PhD, Hiroki Kitaura, DDS, PhD, Ingrid L. Kwee, MD, Tsutomu Nakada, MD, PhD

From the Center for Integrated Human Brain Science Brain Research Institute, University of Niigata (KS, HI, VJH, HK, TN); and Department of Neurology, University of California, Davis (ILK, TN).

ABSTRACT

BACKGROUND

Development of molecular MR imaging (MRI) similar to PET imaging using contrast agents such as gadolinium as probe have been inherently hampered by incompatibility between potential probe (charged molecules) and membrane permeability. Nevertheless, considering the inherent spatial resolution limit for PET of 700μ, the superior microscopic resolution of MRI of 4 μ presents a strong incentive for research into ligand-based molecular MRI.

METHODS

^{17}O exhibits JJ vicinal coupling with a covalently bound proton in a hydroxyl group. This ^{17}O coupled proton can be ionized in water solution and interexchange with other water protons. This property can be utilized as "probe" in T2-weighted imaging and developed into ligand-based molecular MRI. We examined β-amyloid distribution in human APP overexpressed transgenic mice *in vivo* following injection of ^{17}O labeled Pittsburg compound B (^{17}O-PiB).

RESULTS

JJVCPE imaging successfully imaged ^{17}O-PiB, unequivocally establishing that ^{17}O JJVCPE imaging can be developed into PET-like molecular MRI in clinical medicine.

CONCLUSIONS

The study represents the first successful ligand-based molecular MRI *in vivo*. This is also the first *in vivo* amyloid imaging using MRI. High-resolution molecular MRI with high specificity under clinical settings, such as *in vivo* microscopic imaging of senile plaque, is a foreseeable aim.

Keywords: JJ vicinal coupling, amyloid, PiB, Pittsburg compound B, ^{17}O.

Acceptance: Received August 7, 2013, and in revised form November 20, 2013. Accepted for publication December 23, 2013.

Correspondence to: Address correspondence to Tsutomu Nakada, MD, PhD. E-mail: tnakada@bri.niigata-u.ac.jp.

J Neuroimaging 2014;24:595-598.
DOI: 10.1111/jon.12091

Introduction

Molecular imaging refers to imaging techniques capable of visualizing a specific molecule. In clinical medicine, however, it generally implies diagnostic imaging methods of target molecules visualized using an exogenous ligand administered to a patient, and, for a while, it was synonymous to positron emission tomography (PET) imaging.[1] With the rapid technical advancements in diagnostic imaging, especially in the field of magnetic resonance imaging (MRI), the concept of molecular imaging in clinical medicine has been widely expanded.

Molecular imaging using MRI was originally introduced as imaging studies of endogenous molecules such as lactate. This technique is an extension of water suppressed proton spectroscopy based on intrinsic proton signals other than the protons of water and fatty acid side-chains and is commonly referred to as spectroscopic imaging (SI).[2,3] The technique utilizes the intrinsic characteristics of nuclear magnetic resonance (NMR), namely, structure dependent alteration of resonance frequency (chemical shift). Subsequently, this technique was developed into tracer imaging of exogenous ligands containing 19-fluorine, namely, (^{19}F) SI.[4-7] Although a series of publications visualizing metabolic activities of glucose in the brain was the first and, thus far, only successful molecular MRI *in vivo*, technical difficulties precluded its clinical application.

Attempts in developing ligand-based molecular MRI akin to PET imaging using relaxation agents such as gadolinium as probe have been unsuccessful, primarily due to incompatibility between potential probe (charged molecules) and membrane permeability. This is virtually the identical reason why ligand-based molecular imaging has not been developed using computed tomography (CT). This fundamental problem has long precluded effective development of ligand-based molecular imaging in the field of MRI.

The nonradioactive, NMR-sensitive isotope of oxygen, ^{17}O, and adjacent proton will undergo JJ vicinal coupling. In water, the proton of the water molecule and ionized proton of the

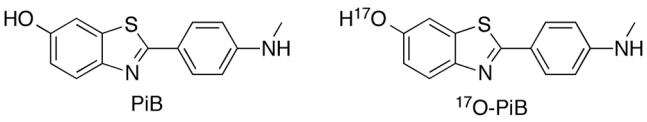

Fig 1. Chemical structures of PiB and ^{17}O-PiB. The hydroxyl group labeled by ^{17}O will be ionized in water and its proton, which vicinal-coupled with ^{17}O, undergoes exchange with water proton, resulting in T2 alteration of adjacent water signals. This process can be detected as intensity change in T2-weighted imaging and, in turn, provides detection of ^{17}O labeled PiB in space.

dissolved molecule will exchange between each other. Therefore, appropriately designed ^{17}O labeled molecules can alter the apparent T2 of adjacent water molecules under nuclear magnetic resonance (NMR) experiments where signal intensity change, δS, can be given by the following equation:[8]

$$\delta S = S_0 \left(1 - \exp\left\{-\mathrm{TE}\left[\frac{1}{\mathrm{T2}} + \frac{35}{12}\rho\tau J^2\right]\right\}\right).$$

Here, S_0 is the original signal intensity, TE, echo time, ρ, relative concentration of ^{17}O labeled substrate, and τ, proton exchange rate.

Although it is difficult to determine the precise concentrations of the ^{17}O labeled target molecule with this method, it is still possible to obtain dynamic data for relative quantification of the target molecule. Using T2-weighted imaging, this technique can be developed into a ligand-based molecular imaging method capable of detecting relative contents of the target molecules labeled by ^{17}O. We explored this technique, referred here to JJ vicinal coupling proton exchange (JJVCPE) imaging,[9] for detecting β-amyloid in transgenic mice that overexpress human APP using ^{17}O labeled Pittsburg-compound B (PiB) (Fig 1).

Materials and Methods

17O-PiB Preparation

Isotopically enriched ^{17}O-methanol (minimum 80%) was obtained from Isotec (St. Louis, MO, USA), and was used as received. Additional reagents were sourced from Sigma-Aldrich (Tokyo, Japan), Wako Pure Chemical Industries (Osaka, Japan), TCI (Tokyo, Japan) and Nacalai Tesque (Kyoto, Japan), and were used as received. Analytical thin-layer chromatography (TLC) was performed using Sigma-Aldrich F254 indicating TLC plates, visualized under UV light, unless otherwise noted. ^{1}H nuclear magnetic resonance (NMR) spectra were recorded at 300 MHz on a Varian Mercury 300 spectrometer (Varian Inc, Palo Alto, CA, USA) and were referenced to an internal tetramethylsilane (TMS) standard. Analytical ultra-performance liquid chromatography (UPLC) and high-resolution mass spectroscopy (HRMS) were performed on a Waters Acquity UPLC (Milford, MA, USA) combined with a Waters LCT Premier XE mass detector, with additional UPLC data obtained using Waters Acquity UPLC PDA and ELS detectors. Exact mass formulae and isotopic distribution correlations were done using ISOMABS (version 5 a, Trace Analysis Research Center, Dalhousie University, NS, Canada).

^{17}O-PiB (80% isotopic enrichment) was prepared starting from ^{17}O-methanol in several steps using standard organic synthetic methods as shown schematically in Figure S1, and as described in the supplemental materials section of the online version of this paper. The chemical properties of the target compound and its key intermediates were in agreement with those previously described for the unlabeled compounds.[10] UPLC analysis of the synthesized ^{17}O-PiB indicated a yield of greater than 98% chemical purity. The product composition was further confirmed by HRMS analysis (mass calculated for C14 H13 N2 OS (M+H+), 257.0749; found, 257.0745). The 17O-isotopic enrichment level of the final product was 84%, calculated on the basis of its mass distribution pattern (M+H+, 18%; M+H++1, 100%; M+H++2, 18%; M+H++3, 6%). Prior to *in vivo* studies, a sample of ^{17}O-PiB was converted to its sodium salt by treatment with an equimolar amount of NaOH in 33% aqueous acetonitrile, which was then lyopholized to give a powdered material suitable for reconstitution into an appropriate vehicle.

JJVCPE Imaging

Animals

The study was carried out in accordance with the animal research guidelines of the Internal Review Board of University of Niigata. Male B6 SJL-Tg (APPSwFlLon, PSEN 1*M 146 L*L 286 V) 6799 Vas/Mmjax mice (1-2 months of age) were obtained from Jackson Laboratory (Bar Harbor, Maine, USA), and raised in our laboratory until 18 months of age.[11] These transgenic mice overexpress both mutant human APP (695) with the Swedish (K670 N, M 671 L), Florida (I716 V), and London (V 717 I) Familial Alzheimer's Disease (FAD) mutations and human PS1 harboring two FAD mutations, M 146 L and L 286 V. Expression of both transgenes is regulated by neural-specific elements of the mouse Thy1 promoter to drive overexpression in the brain.[11] Animals were housed in standard housing conditions with a 12-hour light/dark cycle and were provided with water and food ad libitum.

Mice, spontaneously breathing and anesthetized with an intraperitoneal administration of urethane (1.2 g/kg), were positioned on their backs in a custom-made Plexiglas stereotaxic holder. The head was fixed by ear and tooth bars. Rectal temperature was maintained at 37 ºC ± .5 using a custom designed temperature control system. Oxygen saturation (SpO_2) was monitored throughout the MR measurement using a pulse oxymeter Mouse Ox (STARR Life Sciences Co, Oakmont, PA, USA), with probe placement on the left thigh. A venous catheter was inserted into the right femoral vein for administration of ^{17}O-PiB. Experiments were performed in five transgenic and five wild-type mice.

Imaging Parameters

MRI experiments were performed on a 15-cm bore 7 Tesla horizontal magnet (Magnex Scientific, Abingdon, U.K.) with a Varian Unity-INOVA-300 system (Varian Inc, Palo Alto, CA, USA) equipped with an actively shielded gradient. A custom made one turn surface coil with 20 mm of outer diameter was used for RF transmission. Fast Spin Echo was utilized with the following parameter settings: 1 mm thickness, 256 × 256 matrix image of 16 × 16 mm field, TR 2812 ms, Echo Train 16, Echo Spacing 11 ms, effective TE 88 ms. A total of six scans were

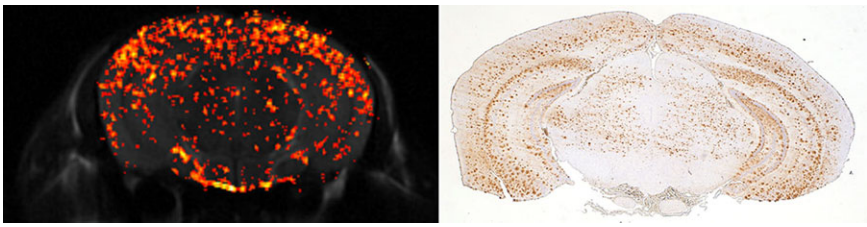

Fig 2. ^{17}O-PiB JJVCPE image of transgenic mouse. Effectiveness of JJVCPE imaging for detecting ^{17}O-PiB in space is clearly demonstrated. Corresponding β-amyloid immune stain histology of the transgenic mouse is shown for comparison. Spatial resolution of the image, ca. 63 μ × 63 μ × 1,000 μ precludes plaque to plaque correlation.

obtained at 30 minutes intervals. 100 mg/kg of ^{17}O-PiB was administrated via venous catheter over 30 minutes starting at the second scan.

Detection of ^{17}O -induced Signal Attenuation

High-resolution T2-weighted images acquired after the administration of ^{17}O-PiB were first corrected for in-plane displacement caused by unavoidable drifts of the MRI system during the long scan time. To shift an MR image at the subpixel level, we applied linear phase modulation to the raw data in k-space along the corresponding direction, based on the following relationship of Fourier transform imaging:

$$F[\exp\{2\pi i(ak_x+bk_y)\}s_{\text{raw}}(k_x,k_y)] = s_{\text{image}}(x-a,\ y-b)$$

where $s_{\text{raw}}(k_x,\ k_y)$ is the raw data of an MRI slice, a and b are the Cartesian shifts (along x and y), $F[]$ represents the Fourier transform, and $s_{\text{image}}(x,\ y)$ the reconstructed slice image without shifting. Note that both s_{raw} and s_{image} are complex-values. We selected the preadministration image as the reference for registration and defined a rectangular region-of-interest (ROI) within it to assess the spatial alignment of postadministration images. The image registration process thus operated in both of the reciprocal domains of Fourier MRI. The position and dimensions of the matching ROI were adjusted to include only a brain region, and the optimum translation parameters were determined as those giving the maximum correlation coefficient of the magnitude values of the pixels, $m = |s_{\text{image}}|$, within the ROI. The correlation maximization was accomplished by Nelder-Mead simplex optimization with initial values $a = b = 0$.

A map of ^{17}O-PiB concentration was then obtained by searching for the maximum of signal attenuation on a pixel-by-pixel basis through the co-registered postadministration images of different acquisition delay times. The map could be represented as $C(x, y) = \max\{d_i(x, y) \mid 1 \le i \le 5\}$ by using the relative signal change $d_i = (m_0 - m_i')/m_0$, where i is the time index of the postadministration image series, m_0 corresponds to the reference, and the prime symbol denotes shift-corrected image. This mapping method was found to be a reasonable workaround for the limitation that the time course of ^{17}O-induced signal change was unknown.

To improve the visibility of small regions of signal variance in the cortex, three types of filters were applied to the map. First, the pixel values in regions not corresponding to brain tissue were nullified by a manually defined binary mask. Without the masking, extremely large signal attenuation ($C >> .1$), particularly seen in the ventricles and near the skin surface, obscured significant but minute signal changes in the cortex by increasing the intensity range of the map. Second, a 2-dimensional Laplacian filter with the following kernel was used for sharpening:

$$U = \begin{pmatrix} 0 & -1 & 0 \\ -1 & 5 & -1 \\ 0 & -1 & 0 \end{pmatrix}$$

This second-derivative filtering, represented as the convolution product (U^*C), increased the contrast of highly localized small differences on the map. Although the kernel U puts larger weight on the center pixel than a typical filter and does not take diagonal pixel values, it appeared to be adequate for the present data.[12] Last, the pixel values of the map were scaled to the range of [0, 1] and threshold set at .5 to remove insignificant components. The survived pixels were color-coded and overlaid onto the gray-scale reference image.

These data processing steps were all conducted using MATLAB R 2009 B (The MathWorks, Natick, MA, USA) on a personal computer equipped with an Intel Core i7 processor.

Immunohistochemistry

Brain tissues were taken from anesthetized mice immediately after the MRI experiments and fixed with 4% paraformaldehyde. The tissues were dehydrated with ethanol and embedded in paraffin wax. Serial sections (10-μm-thick) were cut from the paraffin block and immunostained using mouse monoclonal antibodies against Amyloidβ (IBL, Tokyo, Japan, 1:50). Sections were pretreated with formic acid. Immunolabeling was detected using an avidin-biotin-peroxidase complex method and Vectastain ABC kit (Vector, Burlingame, CA, USA), and visualized with diaminobenzidine/H_2O_2 solution. Counterstaining was carried out with hematoxylin. Specimens were observed using a light microscope (AX 80 T; Olympus, Tokyo, Japan) and images were captured using a digital camera (DP 71; Olympus, Tokyo, Japan).

Results

A representative ^{17}O-PiB JJVCPE image of transgenic mice and corresponding immunohistochemistry are shown in Figure 2. Virtually identical images were obtained for all transgenic mice. For comparison, a representative ^{17}O-PiB JJVCPE image of

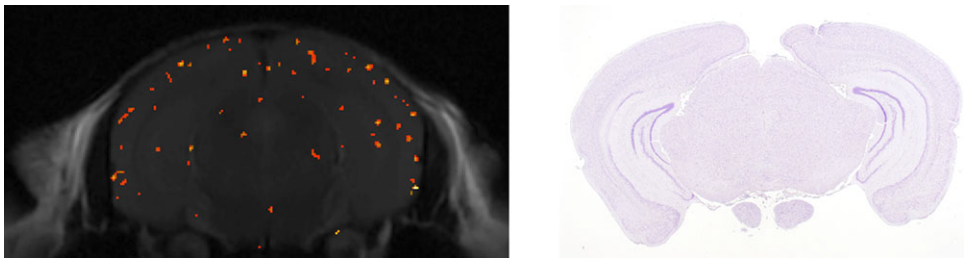

Fig 3. ^{17}O-PiB JJVCPE image of wild type mouse. Nonspecific uptake of PiB is demonstrated as shown before.[15] Corresponding β-amyloid immune stain histology of the wild type mouse is shown for comparison, confirming PiB uptake is nonspecific.

wild type mice showing nonspecific uptake of ^{17}O-PiB and corresponding immunohistochemistry are shown in Figure 3. The spatial resolution of ca. 63 μ × 63 μ × 1,000 μ utilized in this study precludes plaque to plaque correlation. Nevertheless, the effectiveness of JJVCPE imaging for detecting ^{17}O-PiB in space is clearly demonstrated.

Discussion

Pittsburg-compound B (PiB) is a neutrally charged benzothiazole derived from thioflavin T. It was developed into a PET ligand for β-amyloid in 2002. Since PiB PET is ^{11}C based, which has a short half-life of ca. 20 minutes, amyloid imaging by ^{11}C-PiB PET was, in principle, considered investigational.[13,14] Accordingly, the FDA recently approved a longer half-life ^{18}F compound, Florbetapir, for clinical use. Nevertheless, thus far, ^{11}C-PiB PET remains to be the most widely utilized amyloid imaging, and has already provided a great amount of significant clinical information.

PiB has a hydroxyl group, the hydrogen of which is ionized in water solution and exchanged with hydrogen of water molecules. Therefore, the distribution of ^{17}O labeled PiB can be detected with JJVCPE imaging. The current study unequivocally demonstrated that ^{17}O-PiB JJVCPE is capable of detecting amyloid distribution in the brain *in vivo* noninvasively similar to ^{11}C-PiB PET.

This study represents the first successful demonstration of ligand-based molecular imaging using MRI. Although ^{17}O labeling for JJVCPE application is not as flexible as ^{11}C or ^{18}F labeling for PET, considering the relative abundance of hydroxyl group containing bioactive molecules, development of various molecular imaging methods using JJVCPE is realistic. One of the major advantages of MRI over PET is its spatial resolution. While the theoretical limit of spatial resolution for PET is 700 μ, which is due to mean path of positron for annihilation, the theoretical limit for MRI is 4 μ, which is governed by water molecular diffusion. Clinical imaging with microscopic resolution has already been achieved on 7.0 T human systems. The current study confirmed that *in vivo* microscopic analysis of senile plaque in humans is feasible by further refinement of ^{17}O-PiB JJVCPE.

The work was supported by grants from the Ministry of Education, Culture, Sports, Science, and Technology (Japan) and University of Niigata.

References

1. Ido T, Wan C-N, Casella V, et al. Labeled 2-deoxy-D-glucose analogs. ^{18}F-labeled 2-deoxy-2-fluoro-D-glucose, 2-deoxy- 2-fluoro-D-mannose and C-14-2-deoxy-2-fluoro-D-glucose. *J Labelled Compounds Radiopharm* 1978;14:175-182.
2. Luyten PR, Marien AJ, Heindel W, et al. Metabolic imaging of patients with intracranial tumors: H-1 MR spectroscopic imaging and PET. *Radiology* 1990;176:791-799.
3. Maudsley AA, Darkazanli A, Alger JR, et al. Comprehensive processing, display and analysis for in vivo MR spectroscopic imaging. *NMR Biomed* 2006;19:492-503.
4. Nakada T, Kwee IL. Heterogeneity of regional cerebral glucose metabolism demonstrated in situ by 19F FDG NMR rotating frame zeugmatography: one dimensional chemical shift imaging of normal and gliosarcoma implanted brain. *Magn Reson Imaging* 1987; 5:259-266.
5. Nakada T, Kwee IL, Card PJ, et al. 19-Fluorine NMR imaging of glucose metabolism. *Magn Reson Med* 1988;6:307-313.
6. Nakada T, Kwee IL, Griffey BV, et al. 19F NMR glucose metabolic imaging in rabbit. *Radiology* 1988;168:823-825.
7. Nakada T, Kwee IL, Griffey BV, et al. 19F 2-FDG NMR imaging of the brain in rat. *Magn Reson Imaging* 1988;6:633-635.
8. Zhu X-H, Zhang N, Zhang Y, et al. In vivo 17O NMR approaches for brain study at high field. *NMR Biomed* 2005;18:83-103.
9. Nakada T. Grant-in-Aid for Scientific Research: magnetic resonance molecular microimaging. ww.jsps.go.jp/j-grantsinaid/12_kiban/ichiran_21/e.../e07_nakada.pdf
10. Mathis CA, Wang Y, Holt DP, et al. Synthesis and evaluation of C-labeled 6-substituted 2-arylbenzothiazoles as amyloid imaging agents. *J Med Chem* 2003;46:2740-2754.
11. Oakley H, Cole SL, Logan S, et al. Intraneuronal beta-amyloid aggregates, neurodegeneration, and neuron loss in transgenic mice with five familial Alzheimer's disease mutations: potential factors in amyloid plaque formation. *J Neurosci* 2006;26:10129-10140.
12. Castleman KR. Digital image processing. *Prentice Hall* 1996;462-464.
13. Klunk WE, Engler H, Nordberg A, et al. Imaging brain amyloid in Alzheimer's disease with Pittsburgh Compound-B. Ann Neurol 2004;55:306-319.
14. Johnson KA. Amyloid imaging of Alzheimer's disease using Pittsburgh Compound B. *Curr Neurol Neurosci Rep* 2006;6:496-503.
15. Snellman A, Rokka J, Lopez-Picon FR, et al. Pharmacokinetics of [18F]flutemetamol in wild-type rodents and its binding to beta amyloid deposits in a mouse model of Alzheimer's disease. *Eur J Nucl Med Mol Imag* 2012;11:1784-1795.

Supporting Information

Additional Supporting Information may be found in the online version of this article at the publisher's website:

Fig S1. Synthetic scheme for ^{17}O-PiB.